

EPJ Web of Conferences **2**, 10001 (2010)  
DOI:10.1051/epjconf/20100210001  
© Owned by the authors, published by EDP Sciences, 2010

## Effects of nuclear orientation on fusion and fission in the reaction using $^{238}\text{U}$ target nucleus

K. Nishio<sup>1</sup>, H. Ikezoe<sup>1</sup>, S. Mitsuoka<sup>1</sup>, I. Nishinaka<sup>1</sup>, Y. Nagame<sup>1</sup>, T. Ohtsuki<sup>2</sup>, K. Hirose<sup>2</sup>, and S. Hofmann<sup>3,4a</sup>

<sup>1</sup> Japan Atomic Energy Agency, Tokai, Ibaraki 319-1184, Japan

<sup>2</sup> Laboratory of Nuclear Science, Tohoku University, Sendai 982-0826, Japan

<sup>3</sup> Gesellschaft für Schwerionenforschung mbH, D-64220 Darmstadt, Germany

<sup>4</sup> Institut für Kernphysik, Johann Wolfgang Goethe-Universität, D-60486 Frankfurt am Main, Germany

**Abstract.** Fission fragment mass distributions in the reaction of  $^{30}\text{Si} + ^{238}\text{U}$  were measured around the Coulomb barrier. At the above-barrier energies, the mass distribution showed a Gaussian shape. At the sub-barrier energies, triple-humped distribution was observed, which consists of symmetric fission and asymmetric fission peaked at  $A_L/A_H \approx 90/178$ . The asymmetric fission should be attributed to quasifission from the results of the measured evaporation residue (ER) cross-sections for  $^{30}\text{Si} + ^{238}\text{U}$ . The cross-section for  $^{263}\text{Sg}$  at the above-barrier energy agree with the statistical model calculation which assumes that the measured fission cross-section originates from fusion-fission, whereas the one for  $^{264}\text{Sg}$  measured at the sub-barrier energy is smaller than the calculation, which suggests the presence of quasifission.

### 1 Introduction

In the production of superheavy nuclei (SHN) based on the actinide target nuclei and  $^{48}\text{Ca}$  beams [1] the cross-sections do not drop at increasing atomic number, but maintain values of a few picobarn even for the production of the heaviest elements. This makes large difference from cold fusion reactions using lead or bismuth targets [2, 3], where the cross-sections decrease exponentially with atomic number. The relatively large cross-sections for actinide based reactions are explained by a high survival probability of the compound nuclei in competition with fission due to large fission barriers of nuclei in the vicinity of the  $N = 184$  shell closure [1]. Another possible reason could be higher fusion probability. Since nuclei of the actinides are prolately deformed, there exists a configuration where the projectiles hit the equatorial region of the deformed target nuclei. In this case a compact configuration is achieved and the system may have a larger fusion probability than in the reactions using spherical target nuclei of lead or bismuth.

In the reactions with the light projectile  $^{16}\text{O}$  with  $^{238}\text{U}$  target, it is concluded that the system results in fusion even at deep sub-barrier energies from the measured evaporation residue (ER) cross-sections [4]. Fusion occurs from every colliding angle, independently of the nuclear orientation. In the reaction using heavier projectile,  $^{30}\text{Si} + ^{238}\text{U}$ , the measured ER cross-section for  $^{264}\text{Sg}$  at above-barrier energy agrees with a statistical calculation based on the assumption that system captured inside the Coulomb barrier all results in fusion [5]. On the contrary, the cross-section for  $^{264}\text{Sg}$  at the sub-barrier energy are lower than

the calculation, which suggests the presence of fusion hindrance in polar collisions. In this case two different process should be involved in fissions. One is the fission from the fully equilibrated compound nucleus produced in complete fusion. The other is quasifission that system disintegrate without forming a compound nucleus.

The fission fragment mass distributions for the reaction  $^{36}\text{S} + ^{238}\text{U}$  have been measured [6]. In this reaction, we found strong variation of the mass distribution with bombarding energies. At the above-barrier the spectra showed nearly symmetric distribution. In the sub-barrier region, the distribution showed mass asymmetry with the maximum yields at around  $A_H/A_L \approx 200/74$ . We interpreted that the symmetric fission originates from compound-nucleus fission and the asymmetric fission results from quasifission.

We report the measurement of fission fragment mass distributions for  $^{30}\text{Si} + ^{238}\text{U}$  from above- to sub-barrier energies. We expect the asymmetric fission to appear in the sub-barrier region from the measured ER cross-section at the sub-barrier energy.

### 2 Experiment

The fission experiments were carried out at the JAEA tandem accelerator by using the  $^{30}\text{Si}$  beams. The experimental setup is almost the same as in [6]. Beam energies are changed from 191 to 146 MeV to measure the energy dependence of the fragment mass distributions and fission cross-sections. Typical beam intensities were about 0.5–1.0 particle-nA. The  $^{238}\text{U}$  target was prepared by electrodeposition of natural  $\text{UO}_2$  on a Ni backing of  $90 \mu\text{g}/\text{cm}^2$  thick-

<sup>a</sup> Josef Buchmann-Professor Laureatus

This is an Open Access article distributed under the terms of the [Creative Commons Attribution-Noncommercial License](http://creativecommons.org/licenses/by-nc/4.0/), which permits unrestricted use, distribution, and reproduction in any noncommercial medium, provided the original work is properly cited.

ness with a diameter of 5 mm. The thickness of the  $^{238}\text{U}$  contents was about  $80\ \mu\text{g}/\text{cm}^2$ .

Two fission fragments (FFs) were detected in coincidence by using position-sensitive multi-wire proportional counters (MWPCs). The MWPCs have an active area of  $200\ \text{mm} \times 120\ \text{mm}$  in horizontal and vertical direction, respectively. The detectors were located on both sides of the target each at a distance of 211 mm and at angles of  $\theta_1 = -61.0^\circ$  for MWPC1 and  $\theta_2 = +90.0^\circ$  for MWPC2. Each MWPC covers the emission angles of  $-86.0^\circ \leq \theta_1 \leq -36.0^\circ$  and  $65.0^\circ \leq \theta_2 \leq 115.0^\circ$ . For the out-of-plane angle, the MWPC1 covers the range of  $72.0^\circ \leq \phi_1 \leq 108.0^\circ$  at  $\theta_1 = -61^\circ$ , and the MWPC2 covers the range of  $74.1^\circ \leq \phi_2 \leq 105.9^\circ$ . The detectors were operated with isobutane gas at a pressure of about 3 Torr.

The time difference  $\Delta t$  between the signals from two MWPCs were recorded. The signals from both MWPCs contain the information on the energy deposition  $\Delta E_1$  and  $\Delta E_2$  of particles passing through the detectors. The fragment incident position on MWPCs were recorded to give the direction of fragment emission. The folding angle between two fission fragments was used to separate the full momentum transfer (FMT) fissions from fission events following nucleon transfer, which occurs when fissile targets like  $^{238}\text{U}$  are used.

For normalization of the beam current, a silicon surface barrier detector with the solid angle  $1.96\ \text{msr}$  was mounted at  $27.5^\circ$  relative to the beam direction.

### 3 Experimental results and discussions

The cross-sections for the FMT fissions ( $\sigma_{\text{fiss}}$ ) for  $^{30}\text{Si} + ^{238}\text{U}$  are shown in the upper part of Fig.1 as a function of the center-of-mass energy  $E_{\text{c.m.}}$ . The cross-sections are almost equal to those of the projectiles being captured inside the Coulomb barrier ( $\sigma_{\text{cap}}$ ). The cross-section was determined by drawing the angular distribution in the center-of-mass  $85^\circ \leq \theta_{\text{c.m.}} \leq 125^\circ$ , which were fitted to a function in [13] to yield the cross-section. Since the angular range covered in our experiment was limited, so that the  $\sigma_{\text{fiss}}$  values contain an error arising from the uncertainties in  $d\sigma_{\text{fiss}}/d\Omega(\theta_{\text{c.m.}})$  at forward and backward angles. We estimated 28 % uncertainty in  $\sigma_{\text{fiss}}$  in addition to the statistical uncertainty.

The experimental data are compared to the coupled-channels calculations using the code CCDEGEN [7]. The dashed curve is the result without considering any collective properties of target and projectile (one-dimensional barrier penetration model). The dash-dotted curve is the results taking into account the prolate deformation of  $^{238}\text{U}$  with  $\beta_2 = 0.275$  and  $\beta_4 = 0.05$  [8,4]. We have also additionally taken into account the couplings to the  $2^+$  state at 2.235 MeV ( $\beta_2 = 0.316$  [9]) in  $^{30}\text{Si}$  and to the  $3^-$  state at 0.73 MeV in  $^{238}\text{U}$  ( $\beta_3 = 0.086$  [10]), and the results is shown by the solid curve. The experimental data agree with the calculation when the deformation of  $^{238}\text{U}$  was taken into account.

Figure .2 shows the fission fragment mass distributions for  $^{30}\text{Si} + ^{238}\text{U}$ . The fragment masses were determined by using the conservation law for momentum and mass with

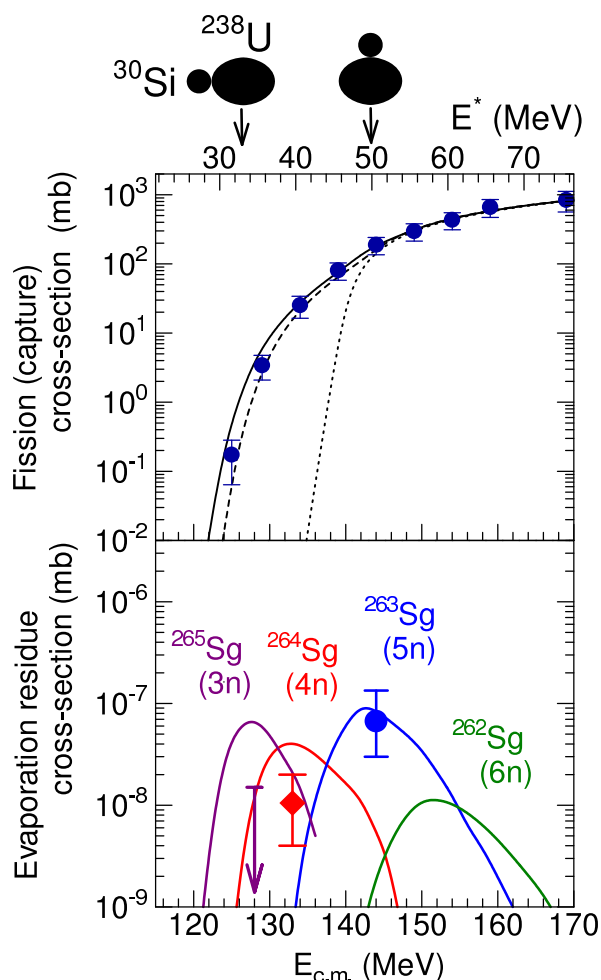


**Fig. 1.** Fission (upper part) and evaporation residue cross-sections (lower part) of the reaction  $^{30}\text{Si} + ^{238}\text{U} \rightarrow ^{268}\text{Sg}^*$  as function of the center-of-mass energy  $E_{\text{c.m.}}$  and excitation energy  $E^*$ . The fission cross-section is obtained in this experiment. The ER cross-section data were from [5]. Curves are the model calculations (see text).

the assumption that mass of the composite system is equal to the sum of those for the projectile and target masses. The distributions are symmetric with Gaussian shape in the energy range from  $E_{\text{c.m.}} = 144.0\ \text{MeV}$  to  $159.0\ \text{MeV}$ , where width of the distribution decreases gradually when beam energy decreases.

At the sub-barrier energies of  $E_{\text{c.m.}} = 134.0$  and  $129.0\ \text{MeV}$ , the distributions have asymmetric component at around  $A_L/A_H \approx 90/178$ . The distribution at  $129.0\ \text{MeV}$  has triple-humped structure because of the enhanced asymmetric fission. Such a structure of asymmetric fission was not observed in the fragment mass distributions for lighter projectile reaction  $^{16}\text{O} + ^{238}\text{U}$  [11], although the standard deviation for the mass distributions increase in the sub-barrier energies. The reaction  $^{26}\text{Mg} + ^{248}\text{Cm}$  also do not show significant asymmetric fission peaks [12]. The data indicates that the projectile  $^{30}\text{Si}$  opens the new fission channel in the sub-barrier energy.

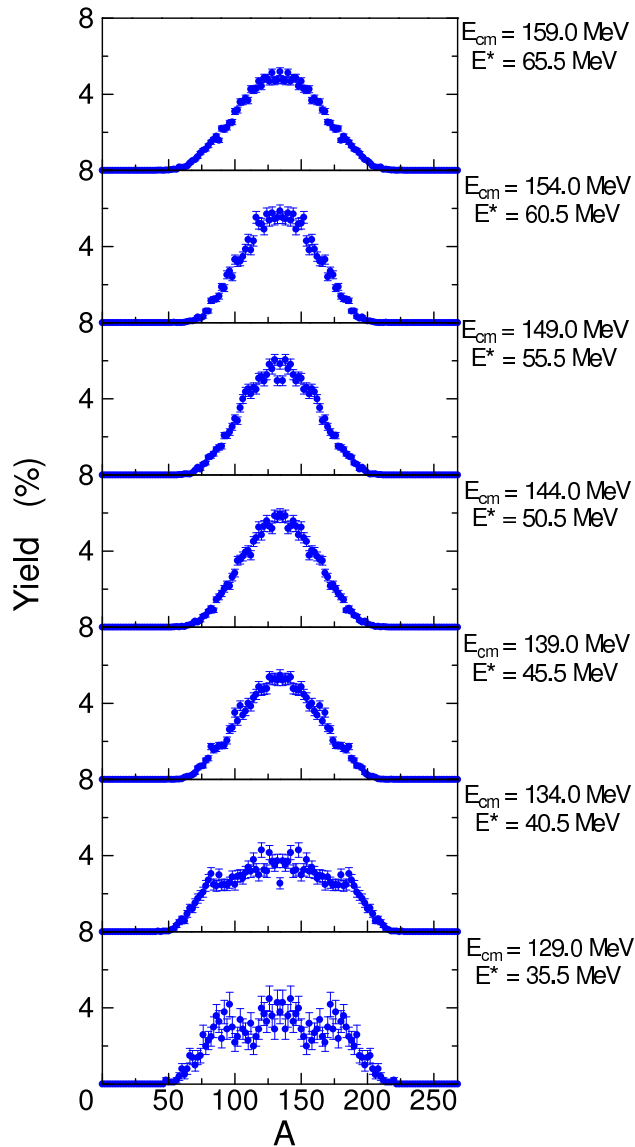


**Fig. 2.** Mass distributions for the full-momentum transfer fissions of the reaction  $^{30}\text{Si} + ^{238}\text{U}$ . The spectra are obtained by normalizing the total yields to be 200%. Reaction energies  $E_{c.m.}$  and excitation energies  $E^*$  of the compound nucleus are given.

The mass distributions for  $^{30}\text{Si} + ^{238}\text{U}$  at sub-barrier energies apparently include different origin in fission which should be attributed to quasifission in order to explain consistently the measured ER cross-sections shown in the lower part of Fig. 1 [5]. The cross-section for  $^{263}\text{Sg}(5n)$  obtained at the above-barrier energy of  $E_{c.m.}=144.0$  MeV agrees with the statistical model calculation (solid curve), which means that fusion is the main process after the system is captured inside the Coulomb barrier and the fragments should originate from the excited compound nucleus. The fragment mass distribution at this energy shows the Gaussian shape typical for the compound nucleus fission. On the other hand, cross-section for  $^{264}\text{Sg}(4n)$  measured at the sub-barrier energy  $E_{c.m.}=133.0$  MeV is about a few factors

of magnitude smaller than the calculation, indicating that quasifission should be involved in the reaction.

The appearance of quasifission in the sub-barrier energies represents the effects of nuclear orientation on fusion and/or quasifission. At the sub-barrier energy, projectile collides on the polar sides of the target nucleus  $^{238}\text{U}$ . The reaction from this configuration has large charge-center distance between the projectile and target nucleus, which results in larger quasifission probability than the reaction starting from the equatorial collisions.

The mass asymmetry of the quasifission for  $^{36}\text{S} + ^{238}\text{U}$  was  $A_L/A_H \approx 74/200$ . The difference could have information for the system approached to the fully amalgamated compound system even when quasifission takes place. Such a model calculation is going based on the fluctuation-dissipation model [14].

## 4 Conclusions

Fission fragment mass distributions in the reaction of  $^{30}\text{Si} + ^{238}\text{U}$  were measured around the Coulomb barrier. In the sub-barrier energies, asymmetric fission at  $A_L/A_H \approx 90/178$  is observed. This is attributed to quasifission from the results of the measured evaporation residue (ER) cross-sections, where the cross-section at the sub-barrier energy is smaller than the statistical model calculation based on the assumption that all the fission events are from compound nucleus formed by fusion. Appearance of the quasifission in the sub-barrier energies indicates that the reaction from the distant touching configuration results in large quasifission probability.

This work was partly supported by a Grant-in-Aid for Scientific Research of the Japan Society for the Promotion of Science.

## References

1. Yu.Ts. Oganessian, *J. Phys. G* **34**, R165 (2007).
2. S. Hofmann and G. Münzenberg, *Rev. Mod. Phys.* **72**, 733 (2000).
3. K. Morita *et al.*, *J. Phys. Soc. Jpn.* **73**, 1738 (2004).
4. K. Nishio *et al.*, *Phys. Rev. Lett.* **93**, 162701 (2004).
5. K. Nishio *et al.*, *Eur. Phys. J. A* **29**, 281 (2006).
6. K. Nishio *et al.*, *Phys. Rev. C* **77**, 064607 (2008).
7. modified version of the CCFULL code, K. Hagino *et al.*, *Computer Phys. Comm.* **123**, 143 (1999).
8. D.J. Hinde *et al.*, *Phys. Rev. Lett.*, **74**, 1295 (1995).
9. S. Raman *et al.*, *At. Data Nucl. Data Tables*, **36**, 1 (1987).
10. R.H. Spear *et al.*, *At. Data Nucl. Data Tables*, **42**, 55 (1989).
11. D.J. Hinde *et al.*, *Phys. Rev. C* **53**, 1290 (1996).
12. M.G. Itkis *et al.*, *Nucl. Phys.* **A787**, 150c (2007).
13. R. Vandenbosch and J.R. Huizenga, *Nuclear Fission* (Academic Press, New York, 1973).
14. Y. Aritomo and M. Ohta, *Nucl. Phys.*, **A753**, 152 (2005).